

# A 90-W Peak Power GaN Outphasing Amplifier With Optimum Input Signal Conditioning

Jawad H. Qureshi, *Student Member, IEEE*, Marco J. Pelk, *Student Member, IEEE*, Mauro Marchetti, *Student Member, IEEE*, W. C. Edmund Neo, *Member, IEEE*, John R. Gajadharsing, Mark P. van der Heijden, *Member, IEEE*, and L. C. N. de Vreede, *Senior Member, IEEE*

**Abstract**—A 90-W peak-power 2.14-GHz improved GaN outphasing amplifier with 50.5% average efficiency for wideband code division multiple access (W-CDMA) signals is presented. Independent control of the branch amplifiers by two in-phase/quadrature modulators enables optimum outphasing and input power leveling, yielding significant improvements in gain, efficiency, and linearity. In deep-power backoff operation, the outphasing angle of the branch amplifiers is kept constant below a certain power level. This results in class-B operation for the very low output power levels, yielding less reactive loading of the output stages, and therefore, improved efficiency in power backoff operation compared to the classical outphasing amplifiers. Based on these principles, the optimum design parameters and input signal conditioning are discussed. The resulting theoretical maximum achievable average efficiency for W-CDMA signals is presented. Experimental results support the foregoing theory and show high efficiency over a large bandwidth, while meeting the linearity specifications using low-cost low-complexity memoryless pre-distortion. These properties make this amplifier concept an interesting candidate for future multiband base-station implementations.

**Index Terms**—Base station, high-efficiency RF power amplifier, mixed-mode amplifier, outphasing amplifier, wideband code division multiple access (W-CDMA).

## I. INTRODUCTION

CURRENTLY, there is high interest from wireless industry in high-efficiency amplifier concepts to accommodate the third generation (3G) and upcoming fourth generation (4G) of communication standards. These new standards offer more and better data services, but to establish this within a restricted frequency band, they make use of signals with high peak-to-average power ratios. As a result, base-station amplifiers operating with these signals will function most of their time, at much lower levels than the peak powers they are designed for.

Consequently, traditional class-AB amplifiers are less attractive candidates for these signals since their efficiency is seriously degraded when operating them below peak power.

Manuscript received January 27, 2009; revised April 30, 2009. First published July 21, 2009; current version published August 12, 2009. This work was supported by NXP Semiconductor and under the PANAMA Research Program.

J. H. Qureshi, M. J. Pelk, M. Marchetti, and L. C. N. de Vreede are with the Electronic Research Laboratory (ELCA), Delft Institute of Microelectronics and Submicrontechnology (DIMES), Delft University of Technology, Delft 2600 GB, The Netherlands (e-mail: j.h.qureshi@ewi.tudelft.nl; m.pelk@tudelft.nl; m.marchetti@tudelft.nl).

W. C. E. Neo and J. R. Gajadharsing are with the RF Innovation Center, NXP Semiconductor, 6534 AE Nijmegen, The Netherlands.

M. P. van der Heijden is with Corporate Information and Technology (I&T), Research, NXP Semiconductor, 5656 AE Eindhoven, The Netherlands.

Color versions of one or more of the figures in this paper are available online at <http://ieeexplore.ieee.org>.

Digital Object Identifier 10.1109/TMTT.2009.2025430

To avoid this efficiency degradation, various amplifier architectures with improved efficiency have been proposed over time. At this moment, two basic concepts seem to be favored, namely, supply-voltage modulation-based methods like envelope tracking [1], envelope elimination and restoration (EER), or polar modulation [1]–[5], as well as load modulation-based concepts, with the Doherty amplifier approach as the overall favorite [6]–[8]. Although both concepts can provide excellent efficiency performance [3], [8], practical implementation of these concepts still have their own specific strong and weak points, e.g., the envelope-tracking amplifier can provide a large RF bandwidth, but is limited for its modulation bandwidth due to speed restrictions in the envelope-tracking hardware. In contrast, Doherty amplifiers can provide a large modulation bandwidth, but are more limited in their RF bandwidth, due to the higher complexity of the RF network. Furthermore, both amplifier concepts typically require the use of expensive digital pre-distortion (DPD) hardware to correct for the memory effects in order to meet the spectral requirements of the communication standards.

In view of this, outphasing amplifiers [9] are generally considered to be easier to pre-distort, while their RF bandwidth can be large compared to Doherty implementations, making them interesting candidates for future multiband multimode base-station operation. However, in spite of their potential, practical outphasing amplifiers are still lacking behind in efficiency performance compared to state-of-the-art envelope tracking [3] or Doherty amplifiers [8].

Nevertheless, outphasing amplifiers [see Fig. 1(a)] have been steadily improved over the last few years. Reported results include outphasing amplifier implementations using DPD [10], outphasing amplifiers with input-power control and differential-phase adjustment for enhanced efficiency performance [11]–[14], as well as outphasing amplifier implementations that feature combinations of input power and phase control with adaptive output-susceptance compensation to enhance the efficiency in power backoff operation [15]. In spite of these promising results, to the authors' knowledge, truly high-power high-efficiency outphasing amplifiers that yield competitive industrial implementations have not yet been brought to light. With this study, we aim to change this situation, by investigating the efficiency limitations of outphasing amplifiers for complex modulated signals, when these are optimally dimensioned and driven with optimum conditioned input signals. Experimental validation is performed through a GaN outphasing circuit demonstrator, which utilizes two independent in-phase/quadrature (I-Q) modulators, to facilitate free-to-choose drive conditions for its branch amplifiers [see Fig. 1(b)]. The resulting amplifier

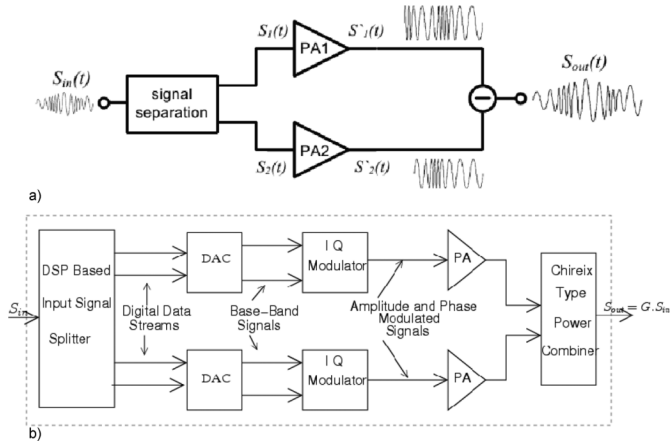


Fig. 1. (a) Block diagram of a conventional outphasing amplifier. (b) LINC amplifier with independent I-Q modulator-based control of the amplifier branches.

provides the highest average efficiency ever reported for an outphasing amplifier operating with a W-CDMA 3G signal, while meeting all linearity specifications [16].

## II. CLASSICAL OUTPHASING AMPLIFIER

In a conventional outphasing amplifier [see Fig. 1(a)], the varying envelope input signal is converted into two antiphase modulated signals with constant envelop. These two signals are amplified by two efficient, but not necessarily linear branch amplifiers. At the output of these amplifying stages, these signals are combined (re)generate the amplified replica of the original input signal (with a varying envelop). Note that by presenting signals with a constant envelop to the branch power amplifiers, AM-AM and AM-PM nonlinearities no longer degrade the linearity of the output signal anymore. This eliminates the linearity requirements of the branch amplifiers, which can now be operated in a high-efficiency mode.

As result, with this concept, linear amplification of the input signal is possible using nonlinear components, explaining its widely used name, i.e., linear amplification using nonlinear components (LINC) [17].

The outphasing amplifier in its original form uses an isolating power combiner to provide high linearity, but its resulting average efficiency is typically not better than that of a simple Class-B amplifier. To improve at this point, Chireix proposed the use of a nonisolating output power combiner [18]. In his approach, outphasing now results in load modulation of the branch amplifiers providing improved efficiency in power backoff operation. Theoretically, a Chireix amplifier has an outstanding performance since, in principle, it can combine high linearity with high efficiency. Unfortunately, practical Chireix amplifier implementations suffer from gain limitations of the branch devices, as well as, their dependence on their dynamically changing complex output loading. These effects result in degradation of their efficiency and linearity [2], [9]. To correct for this efficiency degradation, we will first analyze the optimum input drive conditions of out-phasing amplifiers and their related optimum location of the Chireix compensation points. The linearity of this modified Chireix amplifier will be addressed in Section IV-B through DPD.

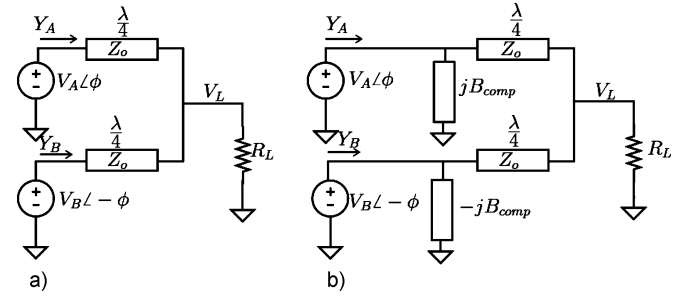


Fig. 2. Chireix transmitter, assuming voltage-source-like operation of the active devices. (a) Without compensation for the complex loading due to outphasing. (b) With compensating shunt susceptance for a specific outphasing angle.

## III. OUTPHASING AMPLIFIER OPTIMIZATION

To investigate optimum outphasing operation, we first consider Fig. 2, which gives a typical Chireix amplifier. Two phase-modulated voltage sources, representing the output stages of branch amplifiers, are connected to a load ( $R_L$ ) by two  $\lambda/4$ -transmission lines, which combine the power delivered by the voltage sources [18]. By controlling the outphasing angle, the output power can be controlled, as well the effective loading of the voltage sources, which yields the high-efficiency operation [18].

Based on the analysis of the circuit schematic in Fig. 2 [2], we can write, for equal amplitudes of  $V_A$  and  $V_B$ , that the power output delivered to the load  $R_L$  is equal to

$$P_{\text{out}} = P_m \cos^2(\phi) \quad (1)$$

with

$$P_m = \frac{R_L}{Z_0^2} (V_A^2 + V_B^2) \quad (2)$$

where  $P_m$  is the maximum output power of the transmitter (2) and  $\phi$  is the outphasing angle between the voltage sources. For the effective shunt admittances, we can write

$$Y_{\frac{\lambda}{4}} = \frac{R_L}{Z_0^2} 2 \cos^2(\phi) \mp j \cdot \frac{R_L}{Z_0^2} \sin(2\phi). \quad (3)$$

As one can observe from (3), the resulting admittances are complex and vary with the outphasing angle. Since active devices provide their highest efficiency when their loading is purely ohmic, it is advantageous to compensate for the variable imaginary part of the load, yielding the well-known reactively compensated Chireix amplifier [18]. In most practical designs, this is done by adding two fixed shunt susceptances to the branches [see also Fig. 2(b)], given by

$$Y_{\frac{\lambda}{4}} = \frac{R_L}{Z_0^2} 2 \cos^2(\phi) \mp j \cdot \frac{R_L}{Z_0^2} \sin(2\phi) \pm j B_{\text{comp}} \quad (4)$$

where  $B_{\text{comp}}$  is

$$B_{\text{comp}} = \frac{R_L}{Z_0^2} \sin(2\phi_c) \quad (5)$$

with  $\phi_c$  being the phase angle for which pure ohmic loading is established. When we assume that the active devices are operating in saturated class-B mode, they tend to behave as voltage

sources [2]. For this situation, the expression for the efficiency [22] of the reactively compensated Chireix amplifier can be written as

$$\eta(\phi, \phi_c) = \frac{\frac{\pi}{4}}{\sqrt{1 + \frac{1}{4} \left( \frac{\sin(2 \cdot \phi_c) - \sin(2 \cdot \phi)}{\cos^2(\phi)} \right)^2}}. \quad (6)$$

Note that the compensation angle  $\phi_c$  should be selected in such a way that the average efficiency of the amplifier is maximized for the signature of the modulated signal under consideration. For clarity, we will assume class-B operation with its related maximum  $\pi/4$  efficiency for the branch amplifiers in the remainder of this paper. The results, however, can be easily renormalized to reflect the use of higher efficiency amplifier classes.

#### A. Selection of the Optimum Compensation Angle for Amplifiers Using Pure Outphasing

To achieve maximum average efficiency for a given envelope modulated signal, the compensation angle must be selected based on the probability density function (PDF) of this signal. For the efficiency optimization of our outphasing amplifier, we will assume W-CDMA operation of which PDF can be described by a Rayleigh distribution [19] at a given peak-to-average ratio (PAR) of the signal ( $\epsilon$ )

$$p(V_n, \epsilon) = 2V_n \epsilon e^{-V_n^2 \epsilon} \quad (7)$$

in which  $V_n$  represents the normalized voltage over the load resistor of our total amplifier. To ease our calculations for this efficiency optimization, we first rewrite the expression for the efficiency (6) in terms of the normalized load voltage ( $V_n = \sqrt{P_L/P_m} = \cos(\phi)$ ), which has a square root relation with the normalized output power

$$\eta(V_n, \phi_c) = \frac{\frac{\pi}{4}}{\sqrt{1 + \frac{1}{4} \left( \frac{\sin(2 \cdot \phi_c) - 2\sqrt{V_n^2 - V_n^4}}{V_n^2} \right)^2}}. \quad (8)$$

Using this notation, the average efficiency of the amplifier can be calculated using (7)–(9) [3], [19], [20], [22].

Consequently,

$$\eta_{\text{avg}}(\phi_c) = \frac{P_{\text{out,avg}}}{P_{\text{dc,avg}}} = \frac{\int_{V_n=0}^{V_n} P_{\text{out}}(V_n) p(V_n) dV_n}{\int_{V_n=0}^{V_n} \frac{P_{\text{out}}(V_n)}{\eta(V_n, \phi_c)} p(V_n) dV_n}. \quad (9)$$

As can be noted, the average efficiency is a function of the compensation angle ( $\phi_c$ ). The optimum value of this compensation angle can be obtained analytically by solving

$$\frac{d(\eta_{\text{avg}})}{d\phi_c} = 0 \quad (10)$$

or graphically by plotting the average efficiency as function of the compensation angle and select the optimum value of  $\phi_c$  for maximum average efficiency [20], [22]. Analytically solving

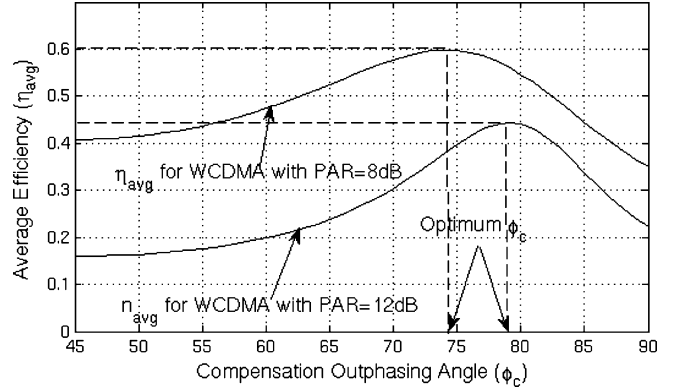


Fig. 3. Average efficiency of the outphasing amplifier for a W-CDMA signal with a PAR of 8 and 12 dB, respectively. The maximum in efficiency sets the optimum outphasing compensation angle.

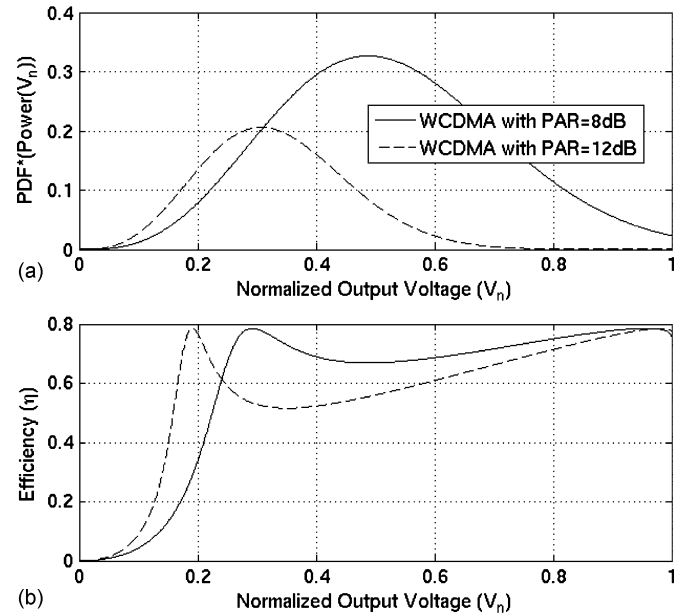


Fig. 4. (a) Power distribution ( $\text{PDF} * \text{Power}(V_n)$ ) of a W-CDMA signal with a PAR of 8 and 12 dB, respectively. (b) Resulting single-tone efficiency as function of normalized output voltage when using the optimum compensation angle for the 8- and 12-dB PAR W-CDMA signals.

(10) is quite tedious so, for simplicity, the graphical approach is given in Fig. 3.

Note that the upper optimization is performed assuming ideal voltage-source-like behavior of the branch amplifier devices, something that will be refined later in Section III-C. In Fig. 4(a), the resulting power distribution is given as function of the normalized output voltage for the 8- and 12-dB PAR wideband code division multiple access (W-CDMA) signals used in the previous optimization. As one can conclude from Fig. 4(a) and (b), the overlap of the power distribution with the single-tone efficiency curve is maximized for these signals when using the optimum compensation angles of  $74^\circ$  and  $79^\circ$ , respectively [see Fig. 4(b)].

#### B. Outphasing Amplifiers Using Input Amplitude Control

After this initial optimization for the average efficiency, we expand the scope of our analysis by considering the possibility to use class-B operation beyond a certain outphasing angle.

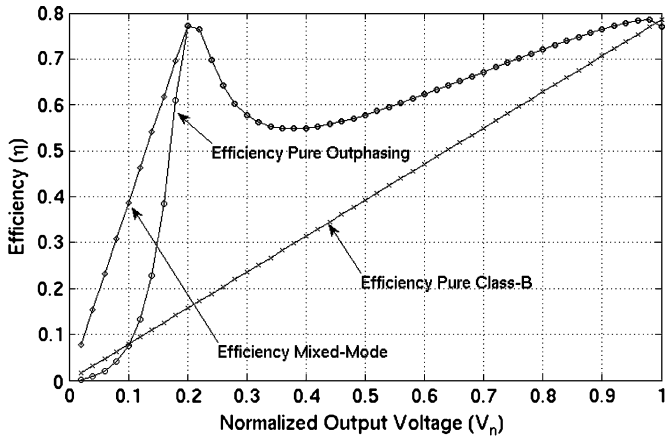


Fig. 5. Efficiency as function of normalized output voltage for a pure class-B amplifier, pure outphasing amplifier, and mixed-mode outphasing amplifier, which uses class-B operation beyond the compensation angle ( $\phi_c = 79^\circ$ ) for the low output power levels to enhance its average efficiency.

The advantage of this mixed-mode operation can be understood when inspecting the efficiency degradation versus increased power backoff of a class-B amplifier in comparison to that of an outphasing amplifier.

For this purpose, we consider Fig. 5, where the efficiency of a traditional class-B amplifier is plotted versus its normalized output voltage. Note that for a class-B amplifier, its efficiency is always linearly proportional with its output voltage. Consequently, its efficiency degradation with increased backoff power is modest. In contrast, when considering the efficiency of a pure Chireix amplifier (8), we also find, besides the desired efficiency peaking in power backoff, a very steep drop in efficiency versus increased backoff power once the outphasing angle is increased beyond the compensation angle  $\phi_c$ . This steep efficiency drop can be explained by the fact that, when using outphasing beyond the compensation angle  $\phi_c$ , the loading conditions of the active devices become almost entirely reactive, something that is very harmful for the efficiency [2]. Due to this phenomenon, pure outphasing amplifiers have a rather low efficiency when operated beyond the compensation angle  $\phi_c$ . Therefore, if the input power and phase of the amplifier branches can be controlled fully independently, it is possible for an outphasing amplifier to switch to class-B operation just a bit beyond  $\phi_c$ . Doing so will result in less reactive loading conditions for the active devices at these low output power levels, while one can benefit from the much lower efficiency roll-off of a class-B operated amplifier. This technique results in significant improvements in average efficiency.

Consequently, using a similar technique as previously used in Fig. 3, it is also possible to estimate the optimum compensation angle for this modified outphasing amplifier and calculate the maximum average efficiency achievable for a W-CDMA signal at a specific PAR. In Fig. 6, the optimum average efficiency with a related optimum compensation angle are plotted for a WCDMA signal as a function of peak-to-average power ratio using the Rayleigh function [19]. Although practical W-CDMA signals normally do not exceed a PAR value of 12 dB, it is chosen here to plot the maximum average efficiency over a larger range to also provide some insight for signals with an

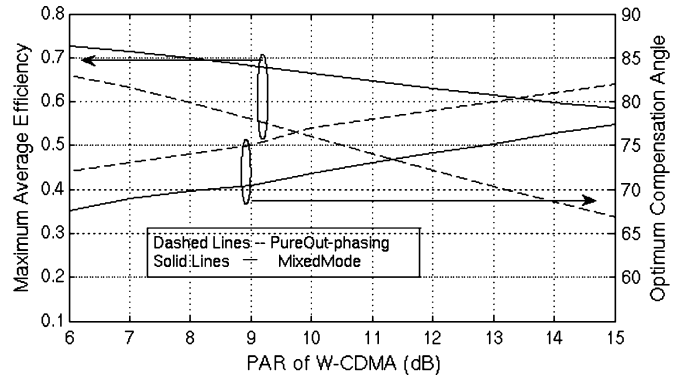


Fig. 6. For a W-CDMA signal as function of PAR, the maximum attainable average efficiency and related compensation angle are given for the pure outphasing amplifier, as well as the mixed-mode operated outphasing amplifier, which utilizes class-B operation at low output power levels to enhance its efficiency.

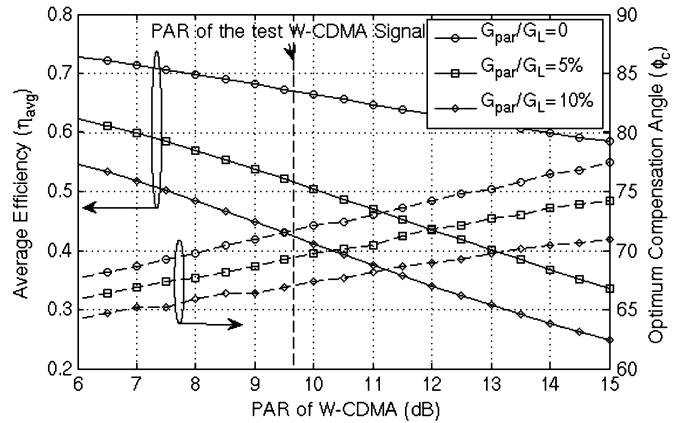


Fig. 7. Maximum achievable average efficiency and related optimum compensation angle of the mixed-mode outphasing amplifier at different ratios of  $G_{par}/G_{opt}$  as function of the PAR of a W-CDMA signal.

even larger PAR. From these results, we can conclude that the use of mixed-mode outphasing/class-B operation yields a significant improvement in average efficiency, e.g., 10% points at a PAR of 11.5 dB, over the conventional pure outphasing-mode operation.

### C. Selection of the Optimum Compensation Angle When Output Losses are Present

Until now, ideal voltage-source-like behavior has been assumed for the amplifying devices. As result, the optimum outphasing angle only depends on the PDF of the input signal. However, when considering practical amplifier implementations, the output stages are loaded by the parasitic shunt conductance of the output devices itself, as well as by the losses in the matching networks and power combiner, yielding a degradation of the efficiency attainable under load modulation. This efficiency degradation will be most pronounced in power backoff, yielding a deviation of the ideal efficiency curves [15]. Consequently, the selection of the optimum compensation angle  $\phi_c$  must also be adjusted. Appendix A discusses the background of this phenomenon in detail. Here, we restrict ourselves to the impact of the output conductance on the average efficiency. For this purpose, Fig. 7 shows the resulting average efficiency

based on the PDF of the W-CDMA signal at various PARs when parasitic loading is present. The results indicate that when parasitic output loading is present, the optimum compensation angle shifts to lower outphasing angles.

With the above, we have concluded our discussion on the theoretical maximum achievable efficiency for the mixed-mode outphasing amplifiers assuming class-B peak efficiency of the active devices. Note when using, e.g., class-F operation for the branch amplifiers, these results need to be renormalized to reflect this particular situation. Since the drain efficiency is an output related quantity, we have based our conclusions on the output behavior of the active devices only. In Section IV, we will focus on how the input signals should be generated to achieve this optimum performance.

#### IV. INPUT SIGNAL GENERATION

In classical outphasing-amplifier implementations, the branch amplifiers are driven by a constant envelope signal such that output devices are always operated in saturation mode, and therefore, closely approximate the behavior of a voltage source. The drawbacks to this approach are the high input power required and a low effective gain that will be achieved in power backoff operation due to this constant input amplitude. As result, the power-added efficiency (PAE) will drop rapidly in power backoff since it is dependent on the RF input power [15]. To improve the PAE, one can make use of the fact that most devices act more like a power-dependent current source than an ideal voltage source. Therefore, the input power needed to drive a device into saturation reduces with the outphasing angle. Consequently, reducing the input power in backoff operation will improve gain, as well as PAE; in addition, it will also avoid excessive overdrive conditions of the active devices that can yield degradation effects [2].

##### A. Optimum Input Signals for Branch Amplifiers

Unlike classical outphasing amplifiers, the input signals for the branch amplifiers of the modified outphasing amplifier contain phase modulation, as well as amplitude modulation, to support the class-B mode in deep power backoff operation. When extending the input power control into the outphasing region, a somewhat more linear relation between input and output power can be established [see Fig. 8(a)]. This approach will yield a more constant and also higher power gain, something that is essential to any successful PA implementation. Consequently, for a particular complex modulated test signal  $S_{in}$ ,

$$S_{in} = r(t)e^{j\theta(t)}. \quad (11)$$

The input signals for the branch amplifiers A and B can be described as

$$S_{PA_{A,B}} = V_{in}(t)e^{j(\pm\phi(t)+\theta(t))} \quad (12)$$

in which

$$\phi(t) = \begin{cases} \text{acos}(r(t)), & \text{if } \text{acos}(r(t)) < \phi_{thr} \\ \phi_{thr}, & \text{if } \text{acos}(r(t)) > \phi_{thr} \end{cases} \quad (13)$$

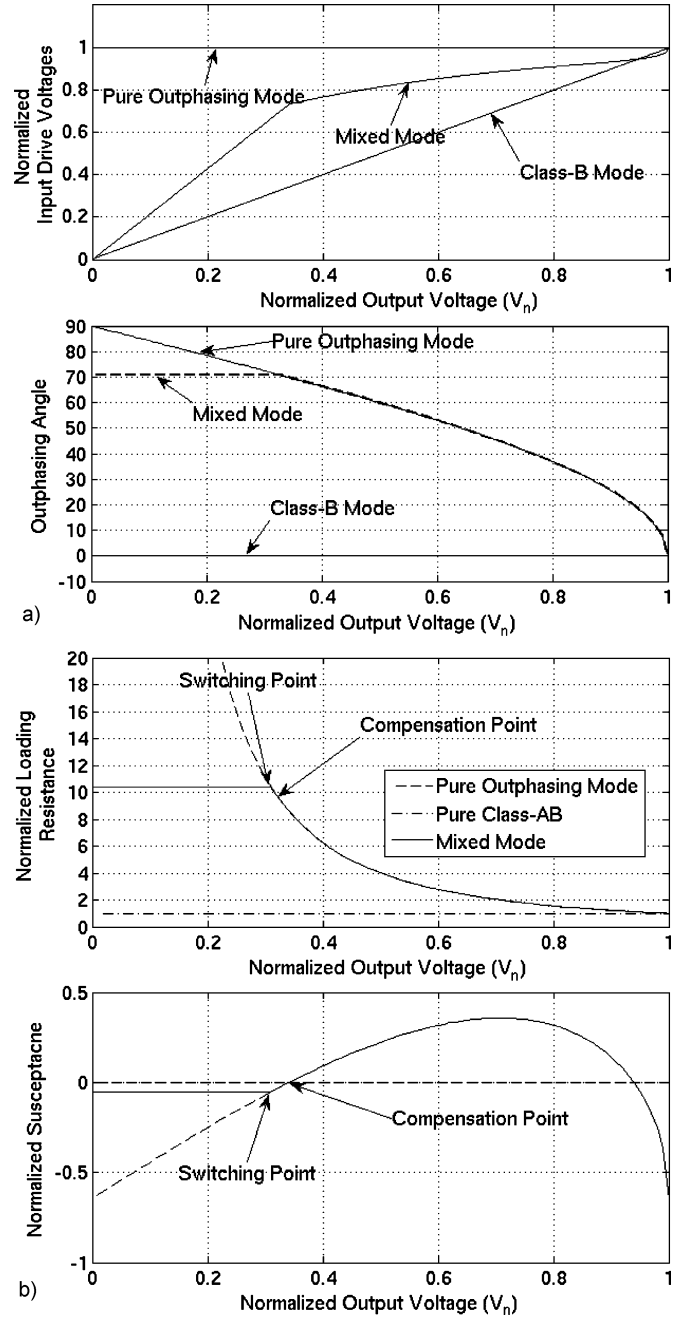


Fig. 8. (a) Input drive voltages and outphasing angles as function of normalized output voltage. (b) Resulting ohmic and reactive loading. (Note that the amplifier is optimized for a PAR of 9.6 dB.)

$$V_{in}(t) = \begin{cases} p_o r(t) + p_1 r^2(t) + p_2 r^3(t) + p_3, & \text{if } \text{acos}(r(t)) < \phi_{thr} \\ \frac{r(t)}{\cos(\phi_{thr})}, & \text{if } \text{acos}(r(t)) > \phi_{thr} \end{cases}. \quad (14)$$

Note that ( $\phi_{thr}$ ) is the outphasing threshold angle where the outphasing mode is changed to class-B operation. The coefficients ( $mp_o, \dots, mp_n$ ) are used to implement the input-power control in the outphasing regime. By controlling the power in this regime, deep compression of the active devices is avoided, something that proves to be beneficial for the gain and PAE of the amplifier (as will become clear later). In the above,  $p_o$  represents the linear term, while the higher order terms ( $p_o, \dots, p_n$ )

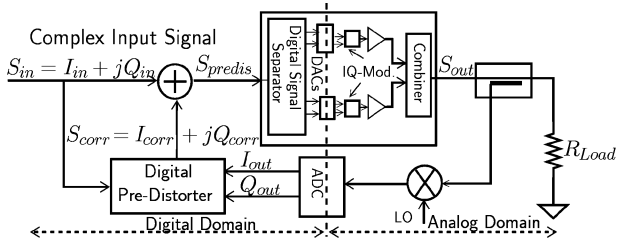


Fig. 9. Principle block diagram of the memoryless closed-loop DPD. Note that the branch signal splitting is done in the digital domain.

are needed to keep the amplifier always a bit in saturated class B when operating in the outphasing mode. The actual value of the parameters ( $p_0, \dots, p_n$ ) are determined by fitting the optimum input power curvature using MATLAB in which the optimum input power curvature is determined experimentally by sweeping both the phase offset between the input signals of the amplifier branches, as well as the power these input signals. The various input drive conditions for the different modes of operation are illustrated in Fig. 8(a). Note that the mixed-mode amplifier operation indeed has a higher input drive than that of a classical class-AB amplifier to enforce the saturated operation of the PA devices in the outphasing regime.

The resulting output loading of the active devices is given in Fig. 8(b). Note that switching to class-B operation indeed limits the reactive loading of the output stages in deep power backoff operation. The real part of the load also no longer increases beyond the level defined by the threshold angle (here,  $\sim 10 \times R_{opt}$ ), which will limit the impact of the output losses in this operation region. Note that the switching is done at the point where the efficiency of the outphasing amplifier drops more rapidly than the class-B amplifier (Fig. 5), which is slightly different than the point where the outphasing amplifier is entirely compensated for the reactive loading. Doing so yields the maximum achievable efficiency at each power level in power backoff operation for the mixed-mode amplifier. However, it must be mentioned that setting  $\phi_{thr}$  equal to  $\phi_c$  will closely approximate this situation in practice. In the actual implementation of our amplifier, the signals for the branch amplifiers will be generated in the digital domain using arbitrary waveform generators (AWGs) in conjunction with two I-Q modulators that up-converted the signals to the RF operation frequency.

## B. DPD

Since the modified outphasing transmitter employs input power and phase control and is only optimized for efficiency, its resulting gain will be nonlinear. Consequently, for fully operational systems, DPD is needed to meet the spectral requirements.

To implement this, we use the basic block diagram of the DPD of Fig. 9. For this constellation-mapping-based DPD algorithm [21], we assume that the mixed-mode outphasing amplifier is a single-input single-output system. This assumption allows pre-distortion to be applied directly on the input signal  $S_{in}$  while the separation for the branch amplifiers is handled in the digital domain by (12)–(14).

As result, the algorithm of pre-distortion can be kept very simple, since it only has to compare the amplified output signal

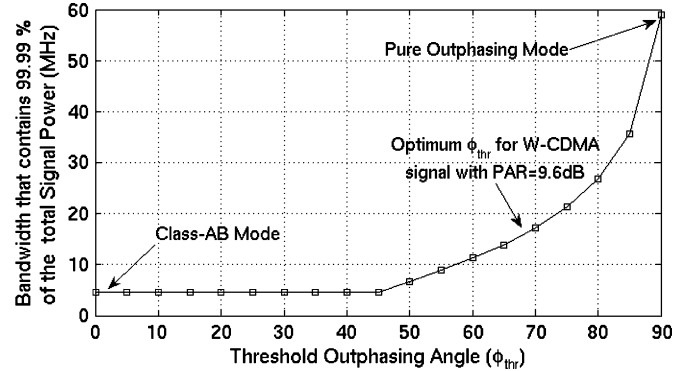


Fig. 10. Bandwidth expansion of the branch amplifiers signal used in a mixed-mode outphasing amplifier as function of threshold outphasing angle for a W-CDMA 3GPP signal with 9.6-dB PAR.

with the original input and adjusts the error terms in the lookup table to make this match as close as possible.

## C. Modulation Bandwidth Expansion

Another important aspect in the design of the PA is the modulation bandwidth used for the branch amplifiers, which is notorious for the classical outphasing amplifier when the original baseband signal is converted to the outphasing signals for the amplifier branches [9]. This expansion is mainly caused by the inverse cosine operation involved in the input-signal processing. Note that this phenomenon not only restricts the modulation bandwidth of the overall transmitter, but also makes the pre-distortion hardware and software more complex and expensive. In addition, due to the bandwidth expansion, memory effects in the branch amplifiers tend to be more pronounced.

In view of this, an additional benefit of mixed-mode amplifier is the very limited bandwidth expansion compared to the classical outphasing amplifier. This can be concluded when considering two extreme cases, namely,  $0^\circ$  and  $90^\circ$  for the outphasing threshold angle. When the threshold outphasing angle is set to zero, the amplifier operates as a pure class-B amplifier and no bandwidth expansion will be present. On the other hand, if the outphasing angle is set to  $90^\circ$ , the amplifier acts like a pure classical outphasing amplifier with related maximum bandwidth expansion (up to a factor of 12 (approximately) for a W-CDMA signal). Therefore, the bandwidth expansion for the mixed-mode amplifier will lie somewhere between these two extremes.

To support the above, a model of the mixed-mode amplifier was developed in MATLAB and operated with a W-CDMA 3G signal, while using different values for the threshold outphasing angle ( $\phi_{thr}$ ). To estimate the bandwidth expansion of the input signals for the branch amplifiers, the bandwidth is plotted for a W-CDMA signal (PAR = 9.6 dB, sampling frequency 122.9 MHz), where 99.99% of the total power is contained. The result is plotted in Fig. 10 and is in line with the above-mentioned expectations. It can be concluded from Fig. 10 that for a 9.6-dB PAR W-CDMA signal, a bandwidth expansion of only a factor of 3.5 can be expected when using the mixed-mode outphasing operation with a threshold angle of  $\phi_{thr} = 68^\circ$ .

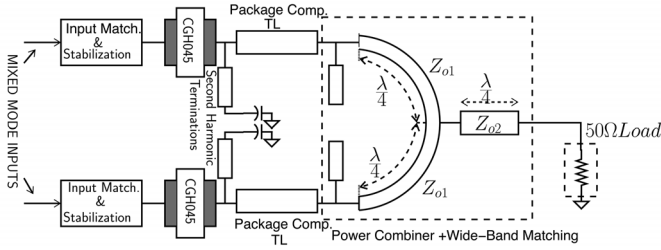


Fig. 11. Simplified schematic of the mixed-mode amplifier.

V. DESIGN OF THE MIXED-MODE OUTPHASING AMPLIFIER

To support the previously introduced theory, a W-CDMA base-station amplifier has been designed that makes use of the proposed mixed outphasing/class-B operation. For the active devices in this demonstrator, two 45-W GaN devices has been used, which, due to their low parasitic output conductance, offer high efficiency even for high-impedance loading conditions. The resulting amplifier provides 90-W peak power (49.5 dBm) at a center frequency of 2.14 GHz.

A. Branch Amplifier Cells

The overall efficiency performance of any outphasing amplifier is determined by its branch amplifiers, which must provide high efficiency not only for optimum loading, but also at the maximum load impedances that occur during outphasing [see Fig. 8(b)]. To guarantee this optimum behavior, the load modulation due to outphasing should correctly transfer to the internal drains of the active devices. Therefore, in the design process, the disturbing influence of package and device parasitic elements (e.g., bond wires and output capacitances) must be compensated. In our design, the influence of these parasitic can be considered as a short artificial transmission line. Consequently, by adding some additional line length, the total effective electrical length can be increased up to 180°.

Note, that for this particular value, the varying load impedance at the output power combiner interface due to outphasing will be perfectly reproduced at the internal drain terminal. Consequently, the output capacitance of the device can also be compensated at the end of this “180° transmission line” (Fig. 11). Device matching for the real part is incorporated in the design of the output power combiner.

Finally, the branch amplifier cells are designed unconditionally stable in order to handle the varying loading conditions due to outphasing without any complication.

B. Chireix Output Power Combiner

The Chireix output combiner is also given in Fig. 11, it utilizes a conventional two-line microstrip power combiner with an additional λ/4 impedance transformer to implement a two-step impedance matching of the branch amplifiers. The resulting low-Q matching results in the required bandwidth for the overall outphasing amplifier.

As final step, based on the theory of the previous sections, which include parasitic output loading, the optimum Chireix compensation angle was found to be 68° for the aimed W-CDMA signal with a 9.6-dB crest factor. The compensation susceptances related to the 68° angle have been combined with

the susceptances needed for the reactive matching of the output capacitances of the active devices. The resulting susceptances are added to the power combiner as open stubs (Fig. 10). Note that, although on first sight the compensation stubs seem to have the same length, in the actual layout, one stub is slightly longer than λ/4, while the other stub is slightly shorter than λ/4 in order to implement the desired compensation susceptances and reactive matching of the active devices.

VI. EXPERIMENTAL RESULTS

A. Test Setup

The block diagram of the test setup is shown in Fig. 12. The baseband signals are generated using Agilent’s high-speed N6030 AWGs and fed to the two I-Q modulators, which deliver the phase and amplitude controlled RF input signals for the branch amplifiers. Additional driver amplifiers are included to bring the input signals to the desired drive power level for the branch amplifiers. To maximize the dynamic range, 10-dB attenuators were inserted in the I and Q paths of the modulators to make use of the full range of the AWGs without overdriving the I-Q modulators.

The output of the mixed-mode outphasing amplifier is fed to a spectrum analyzer and coupled to a mixer. Using a 2.12-GHz local oscillator (LO) signal, this mixer down-converts the 2.14-GHz amplifier output signal to a 20-MHz centered low-IF signal. This signal is sampled by a high data-rate sampling card, while quadrature demodulation is done in the software domain to obtain the I-Q baseband signals that represent the amplifier output. These signals are later used in the digital predistortion to correct for the nonlinearities of the transmitter.

B. Calibration Test Setup

Although DPD is used to correct the amplifier nonlinearities, there are still some effects that cannot be cancelled by the pre-distorter, or greatly impairs its performance. These effects include LO leakage, phase and gain unbalance of the I-Q mixers, as well as gain unbalance in the branch amplifier paths. The actual input power also needs to be known to achieve an accurate estimate of the gain and PAE of the power amplifier.

The LO leakage of the I-Q mixers can be corrected by adjusting the dc-offset voltages of I and Q channels, while the gain unbalance and phase unbalance is corrected using digital compensation [23]. Once the I-Q mixers are calibrated, the gains of the input paths of the mixed-mode amplifier are leveled. To automate these steps, a MATLAB script is written, which determines and stores the correction terms. These terms are later used in the generation of the input signals of the mixed-mode amplifier.

C. Single-Tone Characterization

In the theory sections, we have shown that the efficiency of outphasing amplifiers can be improved by optimizing the power and phase of the input signals. Consequently, to find these optimum input power levels, as well as the optimum threshold angle φ<sub>thr</sub>, a single-tone characterization of the amplifier is performed to estimate the optimum control parameters of (12) and (13). This characterization involves input power sweeps with stepped outphasing angles while measuring the output of the

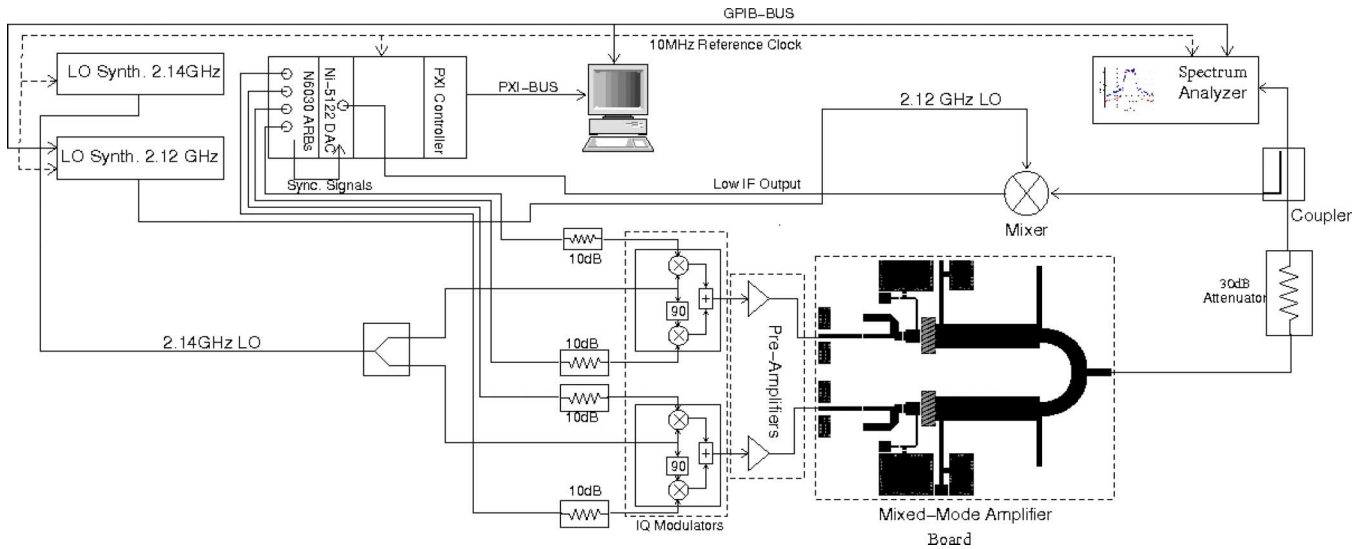


Fig. 12. Block diagram of the measurement test setup for mixed-mode outphasing amplifier.

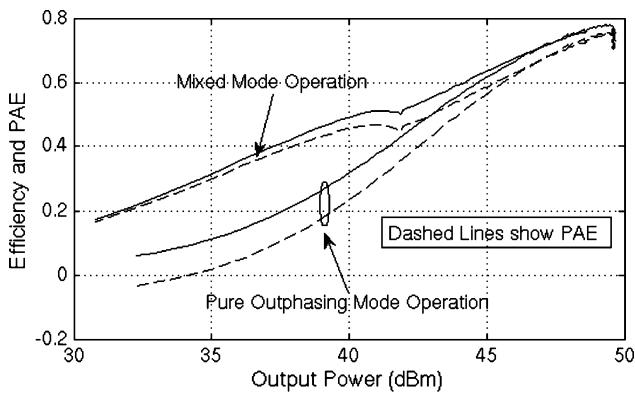


Fig. 13. Measured single-tone efficiency and PAE as a function of output power for the 90-W GaN outphasing amplifier when operated in pure outphasing mode, as well as in mixed outphasing class-B operation.

transmitter. By plotting the maximum achievable efficiency for each output power level, the overall achievable efficiency versus output power is obtained (Fig. 13).

For both cases, the efficiency and PAE of the transmitter in mixed mode, as well as in pure outphasing mode, are measured and plotted. Note, when we operate the amplifier as a pure outphasing transmitter (input power is kept constant), we find the early efficiency roleoff with power backoff, as predicted by the theory. The performance improvements for the mixed-mode operated outphasing amplifier are clearly visible. The input drive conditions used for both cases are shown in Fig. 14. Note that due to the lower input power in mixed-mode operation, the amplifier branches are driven less in saturation, causing a slightly lower output. Consequently, the outphasing angle required in mixed-mode operated amplifiers for a given output power backoff (OPB) level will be slightly lower as reflected by the curves in Fig. 14.

The transducer power gain of the mixed-mode amplifier is plotted in Fig. 15. As can be observed from this figure, there are two distinguishable regions of operation. In the outphasing

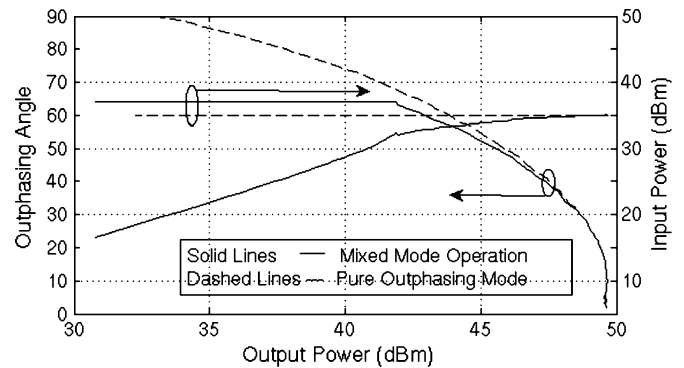


Fig. 14. Input power drive profiles used for the branch amplifiers, in pure outphasing mode, as well in mixed outphasing/class-B operation mode.

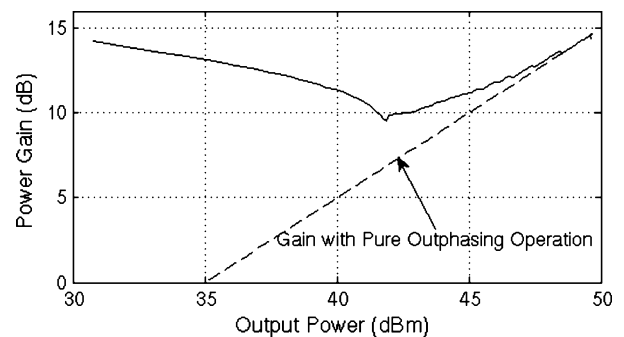


Fig. 15. Measured transducer power gain of the mixed mode amplifier and outphasing amplifier as a function of output power.

mode, the gain reduces with power backoff, but this gain drop is restricted to 4 dB at 8-dB OPB, instead of 8 dB for pure-outphasing operation (Fig. 15). This improved gain is due to the input power control, which is also applied here in the outphasing region. Moreover, when switching to class-AB operation, the gain starts to increase again since the PA devices are coming out of “weak” saturation. Note that we can conclude from Figs. 13 and 15 that pushing class-B operated devices in

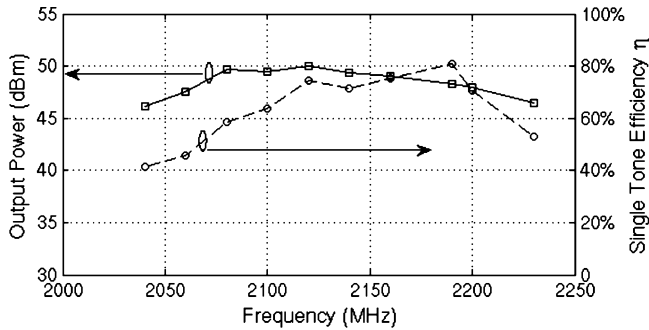


Fig. 16. Measured maximum output power and efficiency as a function of frequency for the 90-W GaN outphasing amplifier.

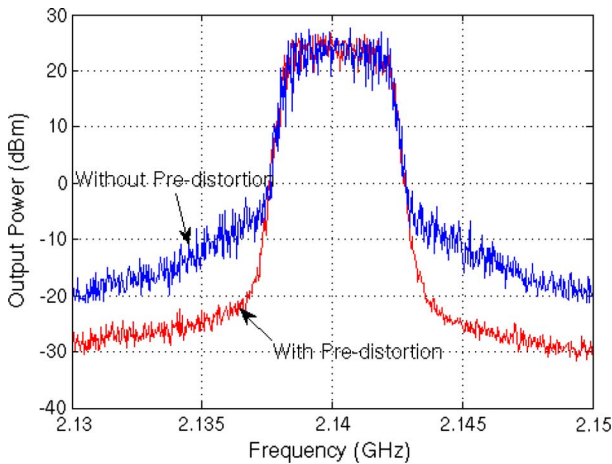


Fig. 17. Measured W-CDMA 3G signal with and without using pre-distorter.

deep compression is harmful for their gain and PAE. This conclusion does not really change when considering saturated operation, e.g., class-E or class-F; here, the inherently lower gain of these classes makes some kind of input power control even more important, when varying the output power over a large range.

The RF bandwidth of the mixed-mode outphasing amplifier has also been investigated. It can be concluded from Fig. 16 that the amplifier is capable of maintaining an output power of more than 48 dBm with high efficiency ( $\eta > 60\%$ ) over a bandwidth of 140 MHz, which is more than sufficient for most broadcast applications.

#### D. W-CDMA Characterization

Once the input power control parameters for the mixed-mode outphasing transmitter are computed, the outphasing amplifier has been tested with a W-CDMA signal with 16 dedicated physical channels (16DPCHs) [16]. The resulting W-CDMA signal has a PAR of 9.6 dB and bandwidth of 3.84 MHz. Fig. 17 shows the output of the transmitter with a W-CDMA signal with and without DPD. Note that the pre-distortion algorithm applied does not correct for memory effects of the amplifier. The resulting measured average power of the pre-distorted output signal is 39.5 dBm, while meeting the spectral requirements for the 3G W-CDMA standard [16]. The related average efficiency for this 9.6-dB crest factor signal is 50.5% and is, to

TABLE I  
PERFORMANCE COMPARISON WITH STATE-OF-ART OUTPHASING AMPLIFIERS

Test Signal	Average Efficiency	ACPR1	ACPR2	Ref
W-CDMA PAR=5.8-7.0dB	20%-30%	41dBc	45dBc	[24]
W-CDMA PAR=7.0dB	42.2%	34.5dBc	35.9dB	[10]
W-CDMA PAR=9.6dB	50.5%	47dBc	51dBc	<b>This Work</b>

the authors' best knowledge, the highest published to date for any outphasing amplifier operated with a W-CDMA signal (see Table I).

#### VII. CONCLUSIONS

In this study, the optimum dimensioning for high-efficiency outphasing amplifiers has been discussed. By making use of class-B operation for the deep power-backoff conditions, extreme loading conditions of the branch amplifiers due to outphasing can be avoided. This results in significant efficiency improvements (in the order of 10%) for complex modulated signals with high peak-to-average power ratios. The impact of output losses for the branch amplifiers has also been considered, yielding refinements of the optimum compensation angles used in the power combining network. For all previous situations, the maximum achievable average efficiency for a W-CDMA signal driven outphasing amplifier is given as function of the applied peak-to-average power ratio. These results indicate that even with class-B operation of the branch amplifiers, average efficiencies for W-CDMA signals in excess of 50%–60% are feasible, provided that the output losses of the active devices and power combiner can be kept low.

Although all efficiency data in this paper is given for (saturated) class-B operation (in the outphasing regime), these results can be easily renormalized to other (higher efficiency) amplifier classes, enabling even better results.

By combining the design strategy of above, with input power backoff for the lower output power levels, the gain and PAE of the total amplifier can also be improved, while excessive overdrive conditions of the active devices with the risk of device degradation can be avoided. It has been shown that the use of the mixed-mode outphasing/class-B operation also proves to be effective in limiting the modulation bandwidth expansion due to outphasing for the branch amplifiers signals. This latter fact will reduce the hardware requirements and cost of the pre-distorter, which can be kept very simple since memoryless pre-distortion can be sufficient to meet the spectral requirements.

All introduced theory is verified using a 90-W peak output power GaN mixed-mode outphasing/class-B operated amplifier. The achieved 50.5% average efficiency for a 9.6-dB crest factor W-CDMA, while meeting the all linearity requirements, is to the authors' best knowledge the highest reported up to date. This, combined with its high-efficiency bandwidth, facilitating multi-channel/multiband operation makes the proposed amplifier concept an interesting candidate for 3G and 4G future communication systems.

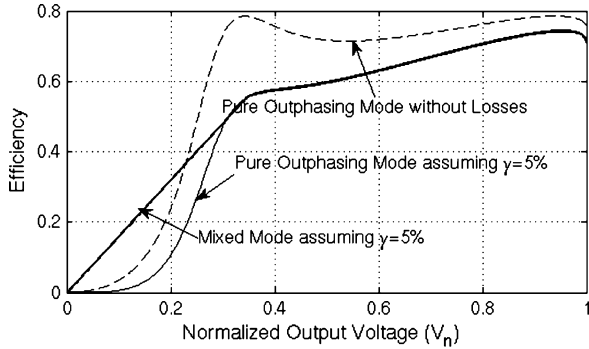


Fig. 18. Efficiency of the outphasing and mixed-mode outphasing amplifier with and without losses.

### APPENDIX A

The parasitic output conductance of the branch amplifiers can be approximated by a conductance connected in parallel with the load [15] with a value given by

$$G_L = G_{\text{opt}} \cdot \cos^2(\phi) \quad (15)$$

where  $G_{\text{opt}}$  is the load conductance seen by the devices when the outphasing angle is equal to zero. By using the relation between normalized output voltage and outphasing angle (Section III-A), the load conductance can be expressed as

$$G_L = G_{\text{opt}} \cdot V_n^2. \quad (16)$$

The decrease of efficiency due to the parasitic conductance depends on the ratio of parasitic output conductance to the load conductance, which increases with outphasing [15], yielding the equation

$$\eta_{\text{lossy}} = \eta_{\text{outphasing}} \cdot \frac{G_L}{G_L + G_{\text{par}}} \quad (17)$$

where  $G_{\text{par}}$  represent the parasitic output conductance.

By using (16) and (17), we write

$$\eta_{\text{lossy}} = \eta_{\text{outphasing}} \cdot \frac{V_n^2}{V_n^2 + \gamma} \quad (18)$$

where  $\gamma = G_{\text{par}}/G_{\text{opt}}$ .

Equation (18) gives the relation of efficiency for the lossy amplifier operated in pure outphasing mode, the same analysis can be extended to the mixed-mode amplifier by considering the fact that, after the threshold outphasing angle ( $\phi_{\text{thr}}$ ), the load conductance is constant, and therefore, the factor

$$\frac{G_L}{G_L + G_{\text{par}}} \Rightarrow \frac{V_{\text{thr}}^2}{V_{\text{thr}}^2 + \gamma} \quad (19)$$

will also be constant. Consequently, the efficiency will follow the ideal class-B roll-off. The resulting relation is

$$\eta_{\text{lossy mixed-mode}} = \begin{cases} \eta_{\text{lossy}}, & \text{if } V_n < V_{\text{thr}} \\ \eta_{\text{lossy}}(V_{\text{thr}}) \cdot \left(\frac{V_n}{V_{\text{thr}}}\right), & \text{if } V_n > V_{\text{thr}} \end{cases} \quad (20)$$

where  $V_{\text{thr}} = \cos(\phi_{\text{thr}})$ , which follows from Section III-A, and  $(V_n/V_{\text{thr}})$  represents the roll-off of a class-B amplifier with output voltage normalized to threshold voltage  $V_{\text{thr}}$ . Equations (16) and (20) are used to create the efficiency curves in Fig. 18.

### ACKNOWLEDGMENT

The authors would like to thank R. Jos, NXP Semiconductor, Nijmegen, The Netherlands, and R. Woltjer, Research at NXP Semiconductor, Eindhoven, The Netherlands. The authors also acknowledge R. Pengelly, T. Dekker, and R. Baker, all with CREE, Durham, NC, for providing the GaN devices with related models.

### REFERENCES

- [1] L. R. Khan, "Single sideband transmission by envelope elimination and restoration," *Proc. IRE*, vol. 40, no. 7, pp. 803–806, Jul. 1952.
- [2] S. C. Cripps, *RF Power Amplifiers for Wireless Communications*. Norwood, MA: Artech House, pp. 113–143, 219–249.
- [3] D. F. Kimball, J. Jeong, C. Hsia, P. Draxler, S. Lanfranco, W. Nagy, K. Linthicum, L. E. Larson, and P. M. Asbek, "High efficiency envelope-tracking W-CDMA base-station amplifier using GaN HFETs," *IEEE Trans. Microw. Theory Tech.*, vol. 54, no. 11, pp. 3848–3856, Nov. 2006.
- [4] F. H. Raab, B. E. Sigmon, R. G. Myers, and R. M. Jackson, "High-efficiency L-band Kahn-technique transmitter," in *IEEE MTT-S Int. Microw. Symp. Dig.*, Jun. 7–12, 1998, vol. 2, pp. 585–588.
- [5] J. Groe, "Polar transmitters for wireless communications," *IEEE Commun. Mag.*, vol. 45, no. 9, pp. 58–63, Sep. 2007.
- [6] W. H. Doherty, "A new high efficiency power amplifier for modulated waves," *Proc. IRE*, vol. 24, no. 9, pp. 1163–1182, Sep. 1936.
- [7] W. C. E. Neo, J. Qureshi, M. J. Pelk, J. R. Gajadharsing, and L. C. N. de Vreede, "A mixed-signal approach towards linear and efficient  $N$ -way Doherty amplifiers," *IEEE Trans. Microw. Theory Tech.*, vol. 55, no. 5, pp. 866–879, May 2007.
- [8] M. J. Pelk, W. C. E. Neo, J. R. Gajadharsing, R. S. Pengelly, and L. C. N. de Vreede, "A high-efficiency 100-W GaN three-way Doherty amplifier for base-station applications," *IEEE Trans. Microw. Theory Tech.*, vol. 56, no. 7, pp. 1582–1591, Jul. 2008.
- [9] X. Zhang, L. E. Lawrence, and P. Asbeck, *Design of Linear RF Outphasing Power Amplifiers*. Norwood, MA: Artech House, 2003.
- [10] I. Hakala, D. K. Choi, L. Gharevi, N. Kajakine, J. Koskela, and R. Kaunisto, "A 2.14-GHz Chireix outphasing transmitter," *IEEE Trans. Microw. Theory Tech.*, vol. 53, no. 6, pp. 2129–2138, Jun. 2005.
- [11] A. Bosma, "Low-loss, asymmetrical combiner for phase differential systems and adaptive RF amplifier comprising an asymmetrical combiner," U.S. Patent WO 2006/064466 A2, Jun. 22, 2006.
- [12] W. Gerhard and R. Knoechel, "Improvement of power amplifier efficiency by reactive Chireix combining, power back-off and differential phase adjustment," in *IEEE MTT-S Int. Microw. Symp. Dig.*, 2006, pp. 1887–1890.
- [13] M. Helaoui, S. Boumaiza, F. M. Ghannouchi, A. B. Kouki, and A. Ghazel, "A new mode-multiplexing LINC architecture to boost the efficiency of WiMAX up-link transmitters," *IEEE Trans. Microw. Theory Tech.*, vol. 55, no. 2, pp. 248–253, Feb. 2007.
- [14] G. Poitau and A. Kouki, "MILC: Modified implementation of the LINC concept," in *IEEE MTT-S Int. Microw. Symp. Dig.*, Jun. 2006, pp. 1883–1886.
- [15] J. Qureshi, R. Liu, A. J. M. de Graauw, M. P. van der Heijden, J. R. Gajadharsing, and L. C. N. de Vreede, "A highly efficient chireix amplifier using adaptive power combining," in *IEEE MTT-S Int. Microw. Symp. Dig.*, 2008, pp. 759–762.
- [16] *3G TS 25.141 Base Station Conformance Testing (FDD)*, 3rd Generation Partnership Project; Tech. Spec. Group Radio Access Netw. Tech. Spec., Rev. V3.1.0, 2000.
- [17] D. C. Cox, "Linear amplification with non-linear components," *IEEE Trans. Commun.*, vol. COM-22, no. 12, pp. 1942–1945, Dec. 1974.
- [18] H. Chireix, "High power outphasing modulation," *Proc. IRE*, vol. 23, no. 11, pp. 1370–1392, Nov. 1935.
- [19] J. F. Sevic, "Statistical characterization of RF power amplifier efficiency for CDMA wireless communication systems," in *Wireless Commun. Conf.*, Boulder, CO, Aug. 1997, pp. 110–113.

- [20] A. Birafane and A. Kouki, "An analytical approach to LINC power combining efficiency estimation and optimization," in *Eur. Microw. Conf.*, Oct. 33, 2003, pp. 1227–1229.
- [21] V. Petrovic, "Reduction of spurious emission from radio transmitters by means of modulation feedback," in *Proc. IEE Radio Spectrum Conservation Tech. Conf.*, Birmingham, U.K., 1983, pp. 44–49.
- [22] F. H. Raab, "Efficiency of outphasing RF power-amplifier systems," *IEEE Trans. Commun.*, vol. 33, no. 10, pp. 1094–1099, Oct 1985.
- [23] X. Huang and M. Caron, "Gain/phase imbalance and DC offset compensation in quadrature modulators," in *IEEE Circuits Syst. Symp.*, 2002, pp. 924–927.
- [24] A. Huttunen and R. Kaunisto, "A 20-W Chireix outphasing transmitter for WCDMA base stations," *IEEE Trans. Microw. Theory Tech.*, vol. 55, no. 12, pp. 2709–2718, Dec. 2007.



**Jawad H. Qureshi** (S'07) was born in Multan, Pakistan in 1976. He received the B.S. degree in electrical engineering from the University of Engineering and Technology, Taxila, Pakistan, in 2000, the M.Sc. degree from the Delft University of Technology, Delft, The Netherlands, in 2006, and is currently working toward the Ph.D. degree at the Delft University of Technology.

From 2000 to 2004, he was with Avaz Networks, Islamabad, Pakistan, where he was involved in digital design. In 2005, he joined the Delft Institute of

Microsystems and Nanoelectronics (DIMES), Delft University of Technology, where he was involved in the design of Adaptive RF circuits and high-efficiency RF power amplifier design. His research interest is in the area of RF PA design.



**Marco J. Pelk** (S'06) was born in Rotterdam, The Netherlands, in 1976. He received the B.Sc. degree in electrical engineering from The Hague Polytechnic, The Hague, The Netherlands, in 2000, and is currently working toward the Ph.D. degree at the Delft Institute of Microsystems and Nanoelectronics (DIMES), Delft University of Technology, Delft, The Netherlands.

In 2000, he joined DIMES. From 2000 to 2002, he was involved in the implementation of compact and mixed-level device models for circuit simulation. Beginning in 2002, he was also involved with the development of a novel active harmonic load-pull system, as well as the design and practical realization of highly efficient power amplifier concepts together with a custom-made measurement setup to characterize its performance. He has authored or coauthored over 15 technical papers. He holds several patents. His current research interests are microwave circuit design, nonlinear device characterization, and radar systems.

Mr. Pelk was a recipient of the 2008 IEEE Microwave Theory and Techniques Society (IEEE MTT-S) Microwave Prize.



**Mauro Marchetti** (S'07) was born in Naples, Italy, in 1981. He received the M.Sc. degree (*cum laude*) in electrical engineering from the University of Naples "Federico II," Naples, Italy, in 2006, and is currently working toward the Ph.D. degree at the Delft University of Technology, Delft, The Netherlands.

Since 2006, he has been with the Delft Institute of Microsystems and Nanoelectronics (DIMES), Delft University of Technology, where he is involved with the development and implementation of advanced characterization setups for RF power amplifiers.



**W. C. Edmund Neo** (S'05–M'08) received the B.Eng. degree in electrical engineering from the National University of Singapore, Singapore, in 2002, the M.Sc. degree in electrical engineering from the Delft University of Technology, Delft, The Netherlands, in 2004, and is currently working toward the Ph.D. degree in electrical engineering at the Delft University of Technology.

His research interest is in the area of novel circuit design techniques for high-efficiency power amplifiers and the design of digital predistorters for linearizing them.

linearizing them.



**John R. Gajadharsing** is currently an RF Power Application Team Leader with NXP Semiconductor, Nijmegen, The Netherlands. He possesses over 20 years of research and development experience in RF power transistor technology and amplifier design for wireless infrastructure. His field of expertise include advanced linearization techniques, high-efficiency amplifier concepts, and advanced system architectures for wireless communication.

Mr. Gajadharsing is a member of the IEEE Microwave Theory and Techniques Society (IEEE

MTT-S).



**Mark P. van der Heijden** (S'00–M'05) was born in Benthuisen, The Netherlands, in 1976. He received the B.Sc. degree in electrical engineering from The Haagse Hogeschool, The Hague, The Netherlands, in 1998, and the PD.Eng and Ph.D degrees in electrical engineering from the Delft University of Technology, Delft, The Netherlands, in 2000 and 2005, respectively.

From 1998 to 2004, he was with the Laboratory of Electronic Components, Technology and Materials, Faculty of Electrical Engineering, Delft University of

Technology, where he was involved with RF amplifier design techniques for linearity and dynamic range. In 2004, he joined the Research Department, NXP Semiconductor (formerly Philips Semiconductor), Eindhoven, The Netherlands. His research interests include high-efficiency power amplifier design and advanced transmitter architectures for wireless communications.



**Leo C. N. de Vreede** (M'01–SM'04) was born in Delft, The Netherlands, in 1965. He received the B.S. degree in electrical engineering from The Hague Polytechnic, The Hague, The Netherlands, in 1988, and the Ph.D. degree from the Delft University of Technology, Delft, The Netherlands, in 1996.

In 1988, he joined the Laboratory of Telecommunication and Remote Sensing Technology, Department of Electrical Engineering, Delft University of Technology. From 1988 to 1990, he was involved in the characterization and physical modeling of ceramic multilayer capacitor (CMC) capacitors. From 1990 to 1996, he was involved with the modeling and design aspects of HF silicon integrated circuits (ICs) for wideband communication systems. In 1996, he became an Assistant Professor with the Delft University of Technology, where he was involved with the nonlinear distortion behavior of bipolar transistors with the Delft Institute of Microelectronics and Nanoelectronics (DIMES). In Winter 1998–1999, he was a guest of the High Speed Device Group, University of San Diego, San Diego, CA. In 1999, he became an Associate Professor responsible for the Microwave Components Group, Delft University of Technology, where he's been involved with RF solutions for improved linearity and RF performance at the device, circuit, and system levels. He has coauthored over 60 IEEE refereed conference and journal papers. He holds several patents. His current interest includes RF measurement systems, technology optimization, and circuit concepts for adaptive wireless systems.

Dr. de Vreede was a corecipient of the 2008 IEEE Microwave Prize.